Cytotechnology (2020) 72:907–919
https://doi.org/10.1007/s10616-020-00436-1

ORIGINAL ARTICLE

Characteristics of apoptosis induction in human breast cancer cells treated with a ceramidase inhibitor

Hüseyin İzgördü · Canan Vejselova Sezer · Emre Çömlekçi · Hatice Mehtap Kutlu

Received: 6 July 2020 / Accepted: 30 October 2020 / Published online: 6 November 2020

Abstract Cancer is a complex disease with high mortality rates. Breast cancer is one of the most fatal diseases both for men and woman. Despite the positive developments on cancer treatment, a successful treatment agent/method has not been developed, yet. Recently, cancer research has been involved in sphingolipid metabolism. The key molecule here is ceramide. Ceramides mediate growth suppress, apoptosis and aging regulation. Ceramidases metabolize ceramide and decrease its level in cells and cause escape the death. Inhibition of ceramidases as new targets for cancer treatment is shown in the literature. Herein, we found that D-erythro-MAPP and its nanoparticle formulation, reduce the viability of MCF-7 cells in a dose-dependent manner with IC_{50} value of 4.4 μM, and 15.6 μM, respectively. Confocal and transmission electron microscopy results revealed apoptotic morphological and ultrastructural changes for both agents. Apoptosis and cell cycle arrest were supported by annexin-V, mitochondrial membrane potential changings and cell cycle analysis, respectively.

Keywords MCF-7 · D-erythro-MAPP · Nanoparticle · Cancer · Sphingolipid

H. İzgördü (✉) · C. Vejselova Sezer · E. Çömlekçi · H. M. Kutlu
Department of Biology, Faculty of Science, Eskisehir Technical University, Eskisehir, Turkey
e-mail: huseyinizgordu@gmail.com

Introduction

Sphingolipids regulate various biological processes such as growth, proliferation, migration, invasion and metastasis by controlling the signal functions within the cancer cell signaling network. Sphingolipid metabolites as ceramide, sphingosine and sphingosine-1-phosphate are involved in controlling cell proliferation and apoptosis. Ceramide and sphingosine production are induced by chemotherapy, radiation or oxidative stress, and these sphingolipids mediate cell death, aging and cell cycle arrest (Ogretmen 2018). Ceramides accumulate in the cell in response to DNA damage, stress, hypoxia and induction of apoptotic molecules (Hannun 1996). The ceramide promotes apoptosis by acting as a negative regulator of cell proliferation. In contrast, sphingosine-1-phosphate (S1P) regulates invasion, angiogenesis as well as processes such as cell growth, survival, and inhibiting apoptosis (Kim et al. 2009). Sphingosine-1-phosphate (S1P) is a suppressive agent of the ceramide-dependent apoptosis mechanism. Therefore, the balance of ceramide and S1P levels in cells is closely related to the fate of cells to survive or die. For this reason, regulation of the ceramidase enzyme and the control of intracellular ceramide, sphingosine and S1P ratios play a key role in the mechanism of apoptosis (Cuvillier 2002). Ceramidase enzymes are drug and radiation-resistant key enzymes that hydrolyze ceramide to produce sphingosine. Because of these

properties, these central enzymes in sphingolipid metabolism have been shown as new targets in the development of cancer treatment strategies and drugs in recent years. Inhibitors of these enzymes have been reported in the literature with excellent potential to develop as new anticancer drugs (Draper et al. 2011). Ceramide also regulates the effects of drugs such as curcumin, resveratrol, nonsteroidal drugs, which are known for their cancer-protective effects. It is stated that these drugs increase the level of ceramides in cancer cells and cause apoptosis (Oskouian and Saba 2010).

In recent years, cancer research has started to take place in sphingolipid metabolism and its relationship with cancer. Breast cancer is a deadly disease both for men and women. The incidence of this cancer in women is higher than in men. The most common cancer in women after lung cancer is breast cancer and ranks second in cancer-related deaths. Breast cancer ranks first among all cancer cases in women in our country with a rate of 24.1%. The incidence and prognosis of this cancer increases by approximately 1.5% every year (Akar et al. 2008). Recently, advances in the early diagnosis and treatment of breast cancer have caused a significant decrease in mortality, while these developments have been insufficient in the treatment of the disease completely. For example, although the number of women surviving breast cancer has increased with early diagnosis, the response rate to therapy is still around 50–60% in patients undergoing chemotherapy treatment for metastatic breast carcinoma. In addition, only 10–15% of patients experienced complete recovery. This low treatment rate is due, among other things, to the inability to understand the mechanism in the pathophysiology of the disease and the lack of new drugs and approaches for treatment. Therefore, the development and use of new therapeutic strategies for cancer treatment and the development of new anticancer drugs are critical (Akar et al. 2008; Koçak et al. 2011). Thus, the key to find a significant target for anticancer therapeutics may be to clarify the role of sphingolipid metabolism especially the balance between ceramide and S1P.

Nanoparticles show much less of the side effects of conventional cancer therapy drugs in cancer treatment. The use of molecules in this form ensures success in treatment. Nanoparticle forms are particles with dimensions of 1–1000 nm. It is stated in the literature that these nanoformulations are generally safe, nontoxic, biocompatible and degradable (Erdoğan 2018; Ateş 2015). Compared to traditional cancer treatments, the size of these nanoparticles allows the drug to be loaded into them to be introduced into the cell in greater quantities and targeted. Because of these properties, the use of anticancer agents in the form of nanoparticles in cancer therapy has a very high potential for a more effective treatment response (Natalie et al. 2009).

Solid Lipid Nanoparticles (SLN) are particles made of solid lipids (solid lipids at room temperature as well as body temperature) and stabilized by surfactants. The main features of SLN's are excellent physical stability, protection of combined unstable drugs against deterioration, controlled drug release (fast/continuous) depending on the merger model, good tolerability and region-specific targeting (Wissinga et al. 2004). The excellence in creating SLN's is the transition to highly regular lipid particles and also the release of the drug (Westesen 2000). These lipids are biocompatible and biodegradable under GRAS (Often Recognized as Safe) status (Das and Chaudhury 2011). SLN's are useful in many ways; the use of organic solvents to produce SLN's can be avoided, their toxicity can be neglected, they can be easily encapsulated with lipophilic compounds, they can be bioavailable with high proportion of lipophilic molecules, and are increased through lymphatic uptake, continuous drug release from the nanoparticle matrix is possible due to the solid nature of matrix leadership and encapsulated drug penetration from the skin or mucous barrier is possible due to the nano-size and to minimize the negative side effects of the molecule (Müller et al. 2002a, b).

Ceramidase inhibitors have been involved in cancer drug research studies in recent years, but the number of studies with (1S,2R)-D-erythro-2-(*N*-myristoylamino)-1-phenol-1-propanol (D-erythro-MAPP) is very low. In addition, no study investigating the efficacy of D-erythro-MAPP's nanoparticle formulation on cancer cells has been found in the literature. In addition, the morphological and ultrastructural changes caused on different cancer cell lines are unknown for D-erythro-MAPP and D-erythro-MAPP SLN compounds. In this study antiproliferative and proapoptotic activities of D-erythro-MAPP as a ceramidase inhibitor and its nanoformulation D-erythro-MAPP SLN formulation were investigated in

human breast cancer cells (MCF-7) including with their cytotoxicity in the morphology and ultrastructure on the test cells.

Material and method

Materials

MCF-7 human breast cancer cells were obtained from the American Type Culture Collection. D-erythro-MAPP, fetal bovine serum, penicillin–streptomycin, dimethyl sulfoxide (DMSO), and 3-(4,5-dimethylthiazol-2-yl)-2,5-diphenyl-2H-tetrazolium bromide (MTT) were obtained from Sigma-Aldrich (USA), and Roswell Park Memorial Institute medium (RPMI-1640) was obtained from GIBCO (USA).

Solid lipid nanoparticle synthesis

The hot homogenization method was used to prepare solid nanoparticles (SLN) loaded with D-erythro-MAPP. In the preparation of SLN, a 3% lipid, 5% D-erythro-MAPP and 1% Tween-80 mixture was used. First, the lipid was dissolved at 80 °C, the substance was added, and then Tween-80 was added, and the substance loaded SLN formulation was obtained by mixing with ultraturaks at 20,500 rpm for approximately 1 min. The obtained suspension are ready to use after cooling and passing through 0.25 µm filters (Cengiz et al. 2016; Baul et al. 2018).

Nanoparticle size, polidispers index measurements and SEM imaging

Zeta size and polidispers index measurements of D-erythro-MAPP loaded solid lipid nanoparticles were made using the Zetasizer Nano Series (Nano-ZS) (Malvern Insturuments, UK). The solid lipid nanoparticles prepared for this process were placed in the cuvette of the device and the conductivity was adjusted to 50 µS with NaCl in distilled water. During the measurements, the temperature of the device was adjusted as 25 °C and the light scattering angle 90°. The shape and morphology of agents were vizualized on a scanning electron microscope (Zeiss Gemini SEM, Germany). For this manner, the samples were placed on separate sample carrier stages and covered with gold (1 min). Covered samples were imaged with SEM (Venkateswarlu and ManJunath 2004).

Cell culture

MCF-7 cells were incubated in RPMI medium containing 10% serum (Fetal Bovine Serum/FBS) and penicillin–streptomycin (100 units/mL) at 37 °C in an incubator containing 5% CO_2 and appropriate humidity standards. The cell medium was replaced each third day with a new RPMI medium. Cells grown in this way were used in experiments after passage 8. It was paid attention that the cells used in the experiments to be confluent by 85%.

MTT assay

The cytotoxicity of D-erythro-MAPP on human breast cancer MCF-7 cells was tested using MTT colorimetric analysis. For this, D-erythro-MAPP stock solution (100 mM) was prepared in DMSO. MCF-7 cells were seeded into 96-well cell culture plates, 5×10^3 cells per well. Cells planted in the plate were incubated at 37 °C and 5% carbon dioxide oven. D-erythro-MAPP and nanoparticle formulation was incubated for 24 h with serial dilution in the concentration range of 3.13–100 µM. At the end of the incubation period, 20 µL of MTT dye (5 mg/mL) was added to the wells and then incubated for 2 more hours at 37 °C. As a result of the incubation, 200 µL of DMSO was added to each well in the well of the plate, and 200 µL of DMSO was added and 570 nm wavelength reading was performed in the HTX-Synergy (Bio-Tek, USA) plate reader. The cell group not treated with D-erythro-MAPP and solid lipid nanoparticle formulation was considered control. Viability values for each dose were calculated according to the control group. The IC_{50} concentration of the applied substance loaded solid lipid nanoparticles on MCF-7 cells was calculated using GraphPad 6.0 using these viability values (Edmondson et al. 1988).

Determination of morphological changes using confocal microscopy

Morphological changes of D-erythro-MAPP and D-erythro-MAPP loaded-SLN formulation on MCF-7 cells were examined by confocal microscopy method. In the preparation phase of MCF-7 cells examined under confocal microscope, cells that were incubated

in 6-well plates with a density of 3×10^5 cells/well were incubated for 24 h with IC_{50} concentrations of D-erythro-MAPP, D-erythro-MAPP loaded-SLN formulations. After 24 h of incubation, the medium was removed, cells were washed in phosphate buffer (PBS) and fixed in glutaraldehyde. After fixation, cells were washed again with PBS and were double-stained with acridine orange and phalloidine dyes, and morphological changes in the cells were examined and imaged using the Leica Confocal Software Version 2.00 software under a confocal microscope (Leica TCS-SP5 II).

Determination of ultrastructural changes using TEM

In order to examine fine structural changes in a transmission electron microscope (TEM), MCF-7 cells with a density of 1×10^6/mL were cultured in a carbon dioxide oven for 24 h, by replicating 12 separate flasks for each group three times. IC_{50} concentrations of D-erythro-MAPP, D-erythro-MAPP-loaded SLN were incubated for 24 h by applying three flasks. At the end of the incubation period, MCF-7 cells were fixed with glutaraldehyde at + 4 °C overnight. After this period, the cells that were washed with buffer were subjected to secondary fixation in osmium tetraoxide. Cells were then dehydrated in ethyl alcohol series (50%, 70%, 90%, 96% and absolute ethyl alcohol). The dehydrated cells were applied with propylene oxide and embedded with resin, and then polymerized in an oven at 60 °C for 48 h. The prepared blocks were thin sectioned (80–100 nm). The prepared thin sections were taken into copper grids and stained in lead citrate and uranyl acetate, then imaging was performed at 120 kV under a transmission electron microscope (Biotwin FEI, USA).

Flow cytometric analyses

Annexin-V staining technique by flow cytometry

For annexin-V analysis, MCF-7 cells were first planted in 6-well plates at 5×10^5 cells in each well and grown for 24 h at 37 °C in a 5% carbon dioxide incubator. MCF-7 cells were incubated for 24 h with IC_{50} concentrations of D-erythro-MAPP, D-erythro-MAPP-loaded SLN. Incubated cells were harvested and washed in PBS. After the cells were washed, 100 µL of cell sample and 100 µL of annexin were added to the flow cytometry tube and incubated for 15 min in the dark at room temperature. Analysis of the samples was performed on the cell analyzer (Muse ™ Cell Analyzer Merck, Millipore, Hayward, California, USA) (Vejselova et al. 2016).

Cell cycle analysis

IC_{50} concentrations of D-erythro-MAPP, D-erythro-MAPP nanoparticles were applied to MCF-7 cells (5×10^5) for 24 h. After the MCF-7 cells were collected in separate tubes, they were centrifuged at 1200 rpm for 5 min, the supernatant was discarded. 250 µL of trypsin buffer solution was added to each tube and mixed gently for 10 min at room temperature. At the end of the period, 200 µL of RNase buffer was added to each tube, mixed gently and incubated for 10 min at room temperature. 200 µL of PI dye solution was added to each tube and mixed gently and incubated in ice for 10 min in the dark in the refrigerator. Cell samples were analyzed on muse Cell Analyzer according to the kit procedure (Muse ™ Cell Analyzer (Merck, Millipore, Hayward, California, USA) (Ciftci et al. 2015).

Evaluation of changes of mitochondrial membrane potential

Mitochondrial membrane potential testing was performed according to the Muse ™ MitoPotential Kit procedure as follows; According to the method studied, Muse ™ MitoPotential working solution was prepared by diluting the MitoPotential Paint 1:1000 with 1 × Test Buffer. For incubation with Muse ™ MitoPotential kit solution, the cells of all the experimental groups were centrifuged after trypsin was applied and ready for the experiment after being suspended with the medium. 95 µL of Muse ™ MitoPotential working solution was added to 100 µL of suspension from the cell sample. Then, it was incubated at 37 °C for 20 min. After incubation, 5 µL of Muse ™ 7-AAD solution was added. Cell samples that were incubated for 5 min at room temperature were analyzed in the Muse ™ Cell Analyzer (Merck, Millipore, Hayward, California, USA) instrument in the mitochondrial membrane potential analysis program.

Statistical analysis

Cytotoxicity test results were tested with one-way analysis of variance (ANOVA) using GraphPad 6.0 program. All tests were analyzed at $p < 0.05$ significance level.

Results

Particle size and polidispers index

The particle size measurements of D-erythro-MAPP and nanoparticle form, the size of D-erythro-MAPP was found to be 830.5 nm, while D-erythro-MAPP-SLN was found to be 15.01 nm ([Average (SD)] (n = 3)). Polydisperse index results of D-erythro-MAPP and nanoparticle formulation showed to be 0.800 for D-erythro-MAPP and 0.387 ([Average (SD)] (n = 3)) D-erythro-MAPP SLN.

Based on the characterization results we obtained in this study, it is revealed that the solid lipid nanoparticles loaded with D-erythro-MAPP are about 55 times smaller in size than the D-erythro-MAPP compound and they have circular shape (Fig. 1).

Cytotoxicity results

D-erythro-MAPP has been shown to reduce significantly the proliferation of MCF-7 cells in a dose-dependent manner. IC_{50} value of D-erythro-MAPP-SLN was determined to be 15.6 µM, while 4.4 µM for the D-e MAPP for 24 h of aplication (Table 1).

It has been observed that the viability of cancer cells decreases depending on the applied agent doses (Figs. 2 and 3).

Confocal microscopy results

It was found that the morphology of MCF-7 cells exposed to IC_{50} of D-erythro-MAPP for 24 h changed significantly compared to control group cells. The nuclei of the control MCF-7 cells and cytoskeleton have a compact structure (Fig. 4). However, morphological changes were detected in MCF-7 cells treated with D-erythro-MAPP and D-erythro-MAPP SLN. These changes are hole formation and fragmentation, chromatin condensation, membrane blebbings in the skeleton (Figs. 4 and 5).

TEM results

TEM findings of MCF-7 cells showed that untreated cells were with normal cytoskeleton, nucleus and cell membrane. Structural changes such as membrane blebbings, holes in the cytoskeleton, chromatin condensation were seen in MCF-7 cells treated with D-erythro-MAPP and D-erythro-MAPP SLN for 24 h (Figs. 6 and 7).

Flow cytometry results

According to annexin-V results, it was determined that MCF-7 control cells were 91.54% alive and 2.01% of the cells died. In this group, the early apoptotic rate was 4.72%, while the late apoptotic rate was 1.73%. In addition, in the annexin-V flow cytometric test results of MCF-7 cells that were exposed to IC_{50}

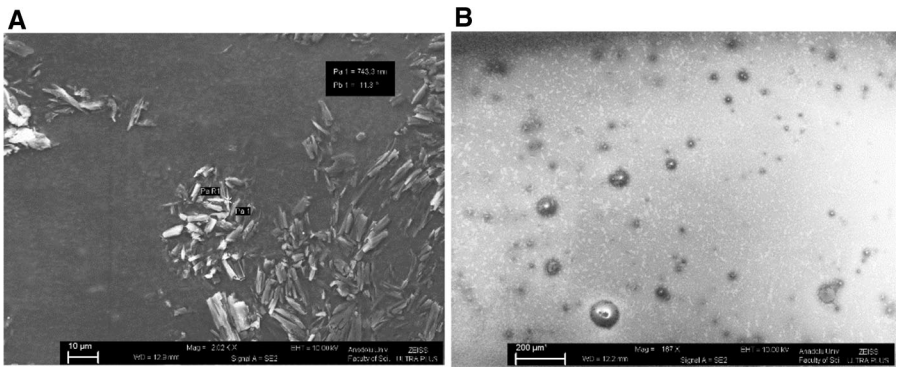

Fig. 1 Morphology of **a** D-erythro-MAPP and **b** D-erythro-MAPP SLN by using scanning electron microscope (SEM)

Table 1 IC_{50} values of MTT test performed by D-erythro-MAPP and D-erythro-MAPP-SLN application on breast cancer cells

Application time (h)	D-erythro-MAPP IC_{50} value (μM)	D-erythro-MAPP-SLN IC_{50} value (μM)
24	4.48	15.65
48	18.84	13.98
72	35.73	12.18

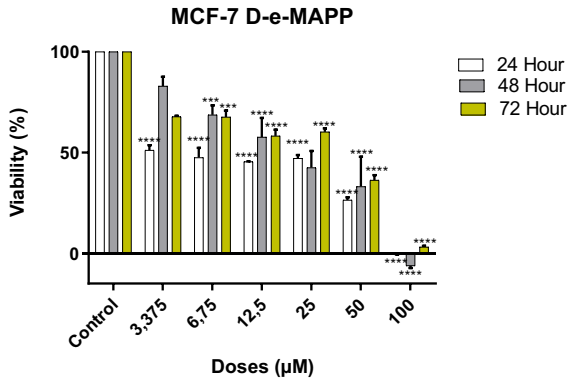

Fig. 2 Viability inhibition of D-erythro-MAPP on MCF-7 cells for 24, 48 and 72 h. IC_{50} values were determined to be 4.4 μM, 18.8 μM and 35.7 μM, respectively. (**** < 0.00001, *** < 0.0001)

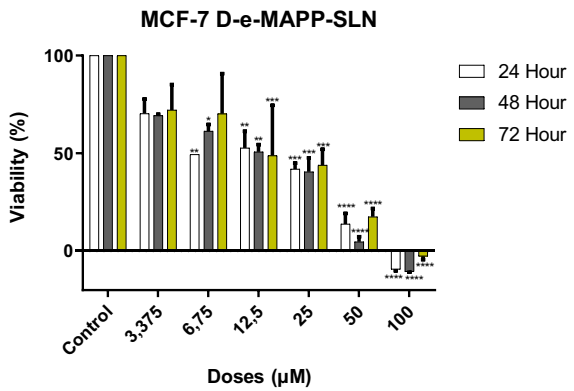

Fig. 3 Viability inhibition of D-erythro-MAPP SLN on MCF-7 cells for 24, 48 and 72 h. IC_{50} values were determined to be 15.6 μM, 13.9 μM and 12.1 μM, respectively (**** < 0.00001, *** < 0.0001, ** < 0.001, * < 0.01)

concentration of D-erythro-MAPP for 24 h, it was determined that dead cells in this group were 3.15%, again when the early apoptotic rate of cells was 25.80% the apoptotic rate was found to be 11.05% (Fig. 8).

It was determined that MCF-7 control cells were 98.83% live and 1.17% of the cells died. In this group, early apoptotic rate and late apoptotic rates were found to be 0.00%. In the flow cytometric test results of the annexin-V activity of MCF-7 cells exposed to the IC_{50} concentration of D-erythro-MAPP SLN for 24 h, the dead cells were 5.41%, while the early apoptotic rate was 10.52% and the late apoptotic rate was 12.23% (Figs. 9).

The cell cycle distribution analysis of untreated MCF-7 cells showed that 86.8%, 5.1%, 5.0% of cells were in G0/G1, S and G2/M, respectively. According to the data cells treated with IC_{50} concentration of D-erythro-MAPP for 24 h were 39.4%, 23.4% and 19.7% in G0/G1, S and G2/M, respectively (Fig. 10).

The cell cycle analysis of MCF-7 control cells showed that 44.8%, 5.5%, 28.0% of cells were in G0/G1, S and G2/M, respectively. According to the data cells treated with IC_{50} concentration of D-erythro-MAPP SLN for 24 h were 24.5%, 3.9% and 22.3% in G0/G1, S and G2/M, respectively (Fig. 11).

It was recorded that MCF-7 control cells found to be 100.00% live/depolarized. 15.95%, 82.35%, 1.7% and 0.0% of MCF-7 cells treated with IC_{50} concentration of D-erythro-MAPP for 24 h were Depolarized/Dead, Dead, Live and Depolarized/Live, respectively (Fig. 12).

Mitopotential measurements of MCF-7 control cells showed that 100.00% were alive. But, MCF-7 cells treated with IC_{50} concentration of D-erythro-MAPP SLN for 24 h were recorded to be 13.95%, 84.60%, 1.70% and 0.05% of were Depolarized/Dead, Dead, Live and Depolarized/Live, respectively (Fig. 13).

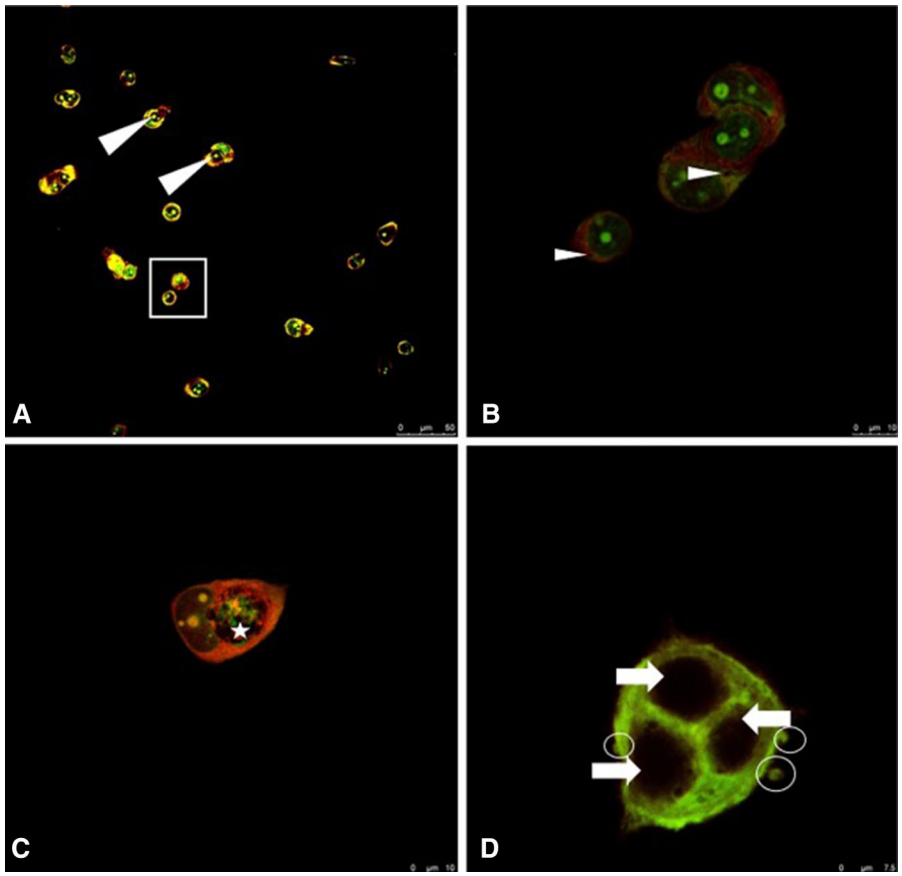

Fig. 4 Confocal microscopy images of MCF-7 cells applied with D-erythro-MAPP. **a** MCF-7 control group cells; Arrowhead: Nucleus, Rectangle: Normal cell structure. **b–d** MCF-7 cells applied with D-erythro-MAPP IC_{50} concentration for 24 h; Asterisk: Hole formation in cell skeleton, Arrow: Condensed nuclei, Arrowhead: Disintegrated cytoskeleton, Circle: Membrane blebbings

Discussion and conclusion

Breast cancer is the most common type of cancer that results in death in women (Siegel et al. 2014). Derived from a patient with metastatic breast cancer in 1970, the MCF-7 cell line was considered as an excellent model system for the study of breast cancer, as it was related to the vulnerability of cells to apoptosis (Yang et al. 2006, Vejselova et al. 2016). In many human tumors, the ceramide level is lower than normal tissue and is inversely proportional to the degree of disease progression. Therefore, stimulating the production of ceramide with various tumor suppression signals encourages cancer cells to apoptosis. Current data suggest that the enzyme pathway that controls intracellular ceramide levels may offer potential new targets for cancer therapy. Ceramides are the most important molecule to the intracellular ceramide pathway (Riboni et al. 2002; Ogretmen and Hannun 2004; Vejselova et al. 2014). Different acid ceramidase inhibitors such as *N*-oleoyl ethanolamine, B-13, DM102, ceranib-2 have been shown to promote apoptosis in many cancers (5RP7), such as prostate, glioma, breast and rat fibroblast cancer (5RP7) (Bhabak et al. 2013; Vejselova et al. 2014).

In this study, cytotoxic, ultrastructural changes and cell death modes caused by a ceramidase inhibitor D-erythro-MAPP and its solid lipid nanoparticle form, which are seen as having high potential for anticancer drug, on human breast cancer cells MCF-7 were investigated. The synthesized nanoparticle formulation was found to be effective in triggering cell death in MCF-7 cells and found to release the drug in time and dose-dependent manner. Our nanoparticle

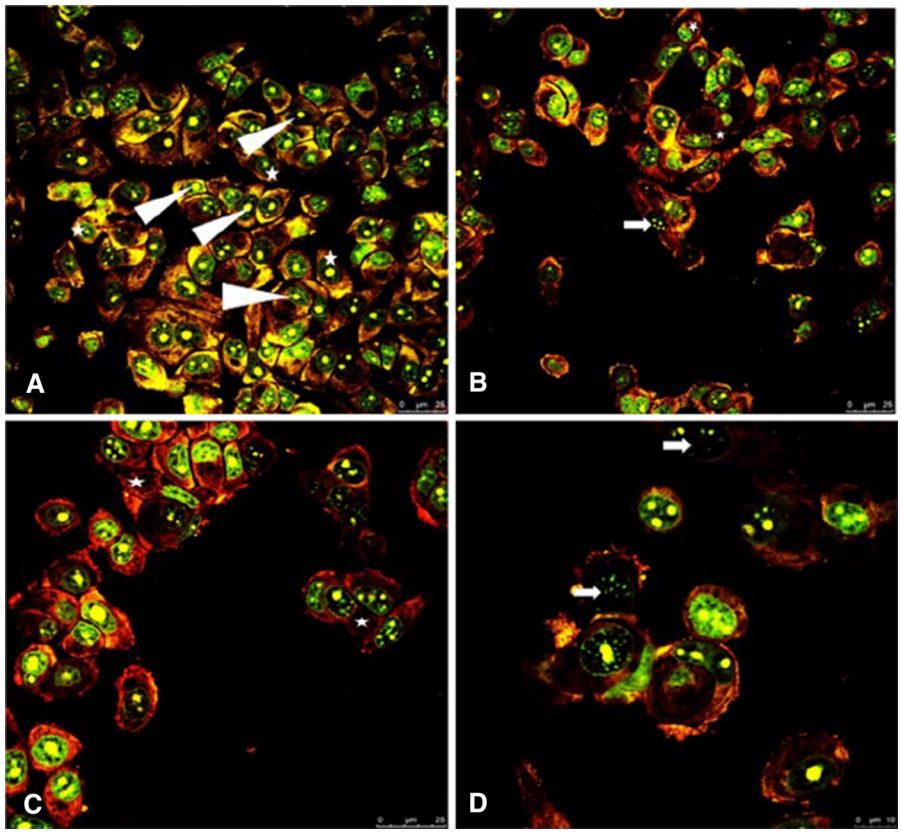

Fig. 5 Confocal microscopy images of MCF-7 cells applied with D-erythro-MAPP SLN. **a** MCF-7 control cells; Arrowhead: nucleus, Asterisk: normal cell structure. **b–d** MCF-7 cells applied with IC_{50} concentration of D-erythro-MAPP SLN for 24 h; Asterisk: hole formation and disintegration in cell skeleton, Arrow: fragmented nuclei

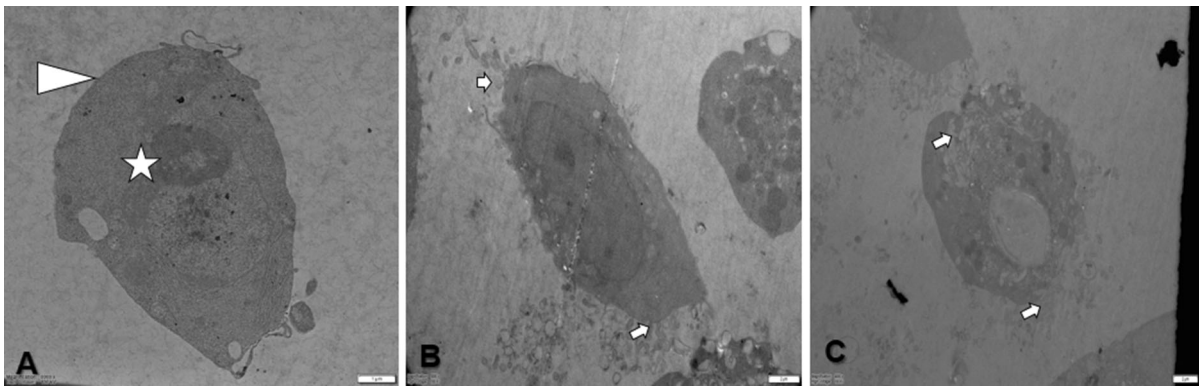

Fig. 6 TEM images of MCF-7 cells exposed to IC_{50} concentration of D-erythro-MAPP for 24 h. **a** MCF-7 control cells; Arrow: normal cell membrane, Asterisk: normal cytoskeleton, **b** and **c** MCF-7 cells exposed to IC_{50} concentration of D-erythro-MAPP, Arrow: membrane blebbing

characterization analysis results D-erythro-MAPP-SLN confirmed that the particle size was about sixty-two times smaller than normal D-erythro-MAPP. Moreover, our SEM findings supported our zeta size analysis results (Fig. 1). In addition, it has been observed that the shape of nanoparticles are spherical and smooth morphologically (Fig. 1). MTT cytotoxicity test results indicated growth supression by both

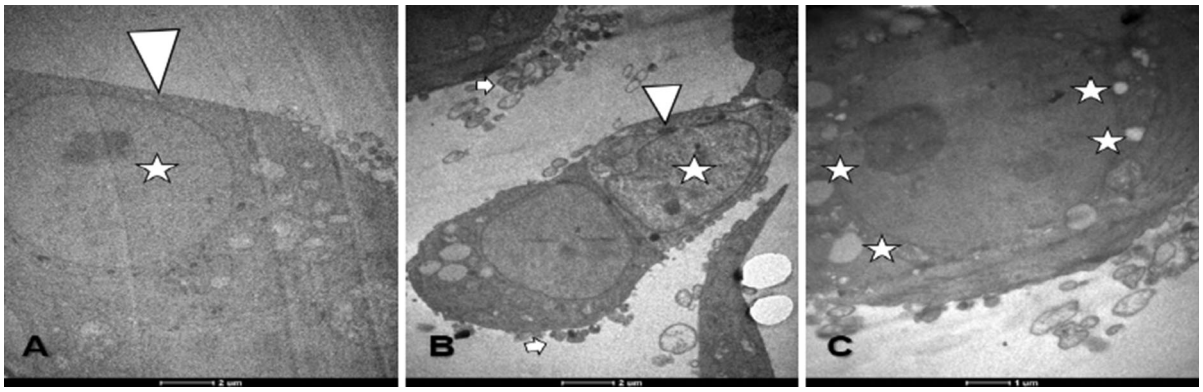

Fig. 7 TEM images of MCF-7 cells exposed to IC_{50} concentration of D-erythro-MAPP nanoparticle form for 24 h. **a** MCF-7 control cells; Arrow: normal cell membrane, Asterisk: normal cytoskeleton, **b** and **c** D-erythro-MAPP MCF-7 cells exposed to IC_{50} concentration of nanoparticle form, Arrow: membrane buds, Asterisk: holes in cytoskeleton, Arrow-head: chromatin condensation

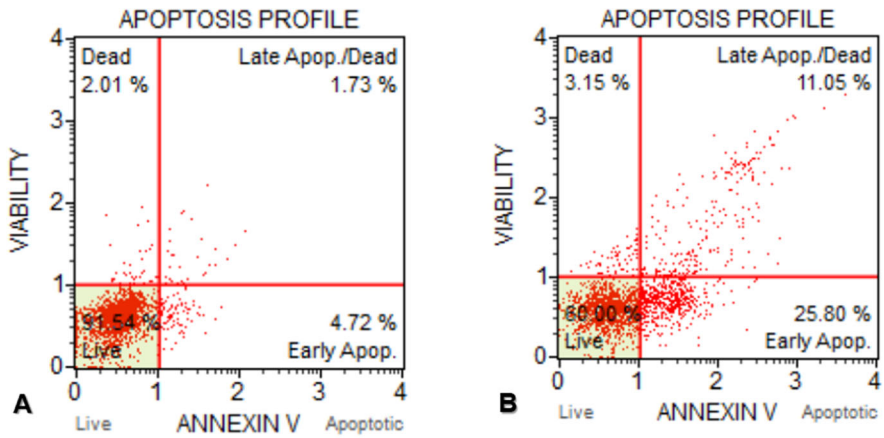

Fig. 8 Annexin-V test results of MCF-7 cells exposed to IC_{50} concentration of D-erythro-MAPP for 24 h. **a** MCF-7 control cells, **b** MCF-7 cells exposed to IC_{50} concentration of D-erythro-MAPP for 24 h

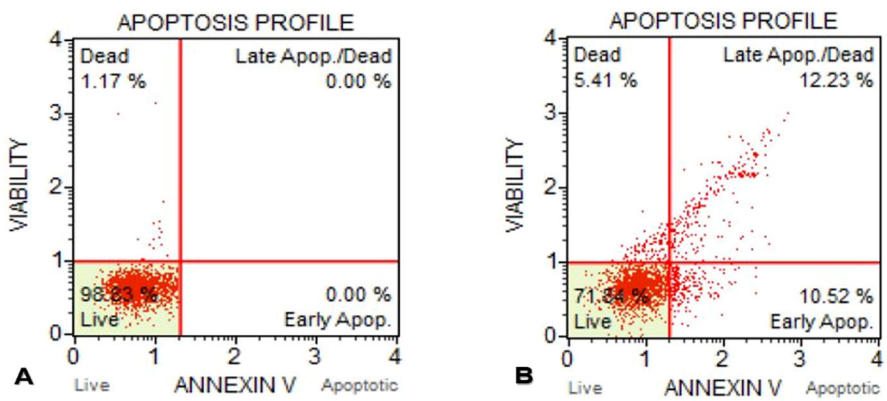

Fig. 9 Annexin-V test results of MCF-7 cells exposed to IC_{50} concentration of D-erythro-MAPP SLN for 24 h. **a** MCF-7 control cells, **b** MCF-7 cells exposed to IC_{50} concentration of D-erythro-MAPP SLN for 24 h

agents applied to the MCF-7 cells but SLN formulation exherted dose and time dependency of cytotoxicity while D-erythro-MAPP showed its cytotoxicity onlu in dose dependent manner. These data imply to the conrolled drug resease property of the synthesized D-erythro-MAPP SLN and availability of D-erythro-MAPP agent for short-time applications. It was determined that the most effective application time

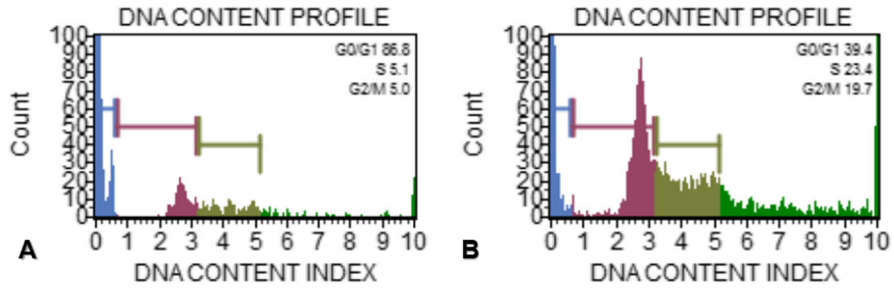

Fig. 10 Cell cycle distribution of MCF-7 cells exposed to IC_{50} concentration of D-erythro-MAPP for 24 h. **a** Control cells **b** MCF-7 cells exposed to IC_{50} concentration of D-erythro-MAPP show blue color flow, green color S phase, light green color G2/M phase and red color G0/G1 phase. (Color figure online)

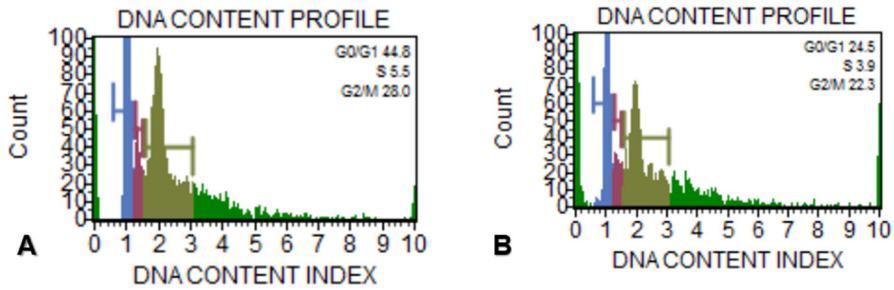

Fig. 11 Cell cycle distribution of MCF-7 cells exposed to IC_{50} concentration of D-erythro-MAPP SLN for 24 h. **a** Control cells **b** D-erythro-MAPP MCF-7 cells exposed to the IC_{50} concentration of the nanoparticle form indicate Blue color flow, green color S phase, light green color G2/M phase and red color G0/G1 phase. (Color figure online)

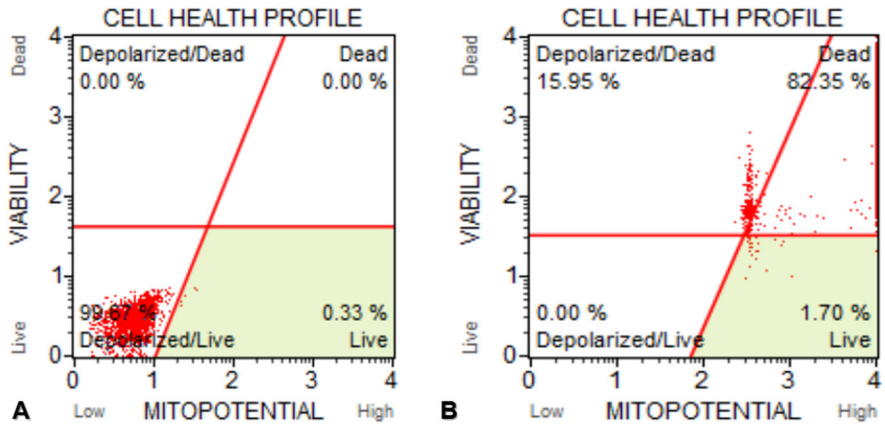

Fig. 12 Results of mitochondrial membrane potential changes of MCF-7 cells exposed to IC_{50} concentration of D-erythro-MAPP for 24 h. **a** Control cells, viability rate was determined as 100.00%. **b** MCF-7 cells exposed to IC_{50} concentration of D-erythro-MAPP were determined as 82.35% of dead cells

of D-erythro-MAPP was 24 h, while this time was 72 h for the nanoparticle formulation accompanied with its time and dose dependency. Zdzislaw et al. in their study in 2008, found the effectiveness of D-erythro-MAPP in MCF-7 cells at the end of 48 h, IC_{50} value as 30 µM (Zdzislaw et al. 2008). In another study, D-erythro-MAPP was reported to inhibit selectively AlkCDase isolated from HL-60 human promyelocytic leukemia. The agent's IC_{50} value is 1–5 mM and has been reported to suppress concentration and time-dependent growth Bielawska et al. (1996). Choi et al. (2003) showed in their study that the expression of neutral ceramidase is expressed at a high level in mesengial cells. The researchers stated that neutral ceramidase inhibition performed by D-erythro-MAPP increased ceramide levels in cultured mesengial cells

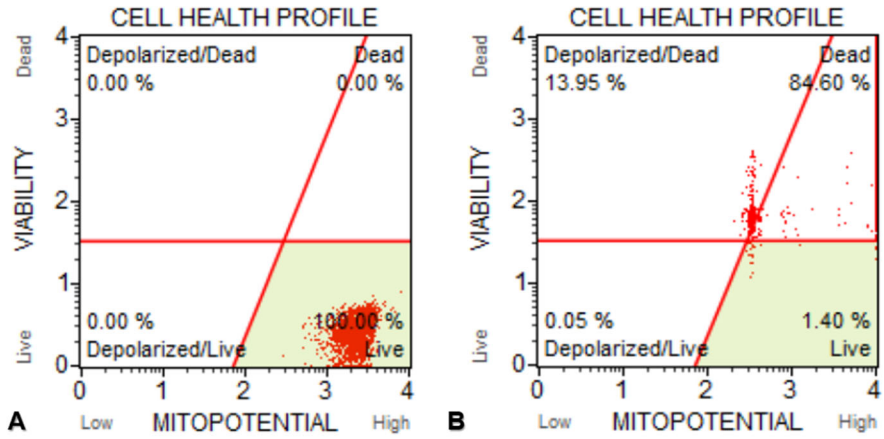

Fig. 13 Results of mitochondrial membrane potential changes of MCF-7 cells exposed to IC_{50} concentration of D-erythro-MAPP SLN for 24 h. **a** Control cells, the viability rate was determined as 100%. **b** MCF-7 cells exposed to IC_{50} concentration of the D-erythro-MAPP SLN, the ratio of dead cells was determined as 84.60%

and in certain areas of the mouse small intestine, resulting in apoptotic cell death.

Cell shrinkage, chromatin condensation and nuclear fragmentation are some of the morphological hallmarks of apoptosis (Vethakanraj et al. 2015). Similar morphological changes were observed in this study as potential anticancer effects of D-erythro-MAPP and D-erythro-MAPP SLN on human breast cancer MCF-7 (Figs. 4 and 5). The obtained morphological analysis results indicated to clearly apoptotic death pattern and where considered as signs of potential anticancer activities of the agents on MCF-7 cells, excessievly for the D-erythro-MAPP SLN formulation.

At Figs. 6 and 7 were shown ultrastructural changes on MCF-7 cells exposed to both agents. The findings were in compatibility with our confocal microscopy findings and underlined the induced apoptotic pathway by the applied agent being more effective in MCF-7 cells exposed to D-erythro-MAPP SLN. Another important feature of apoptosis is the loss of membrane symmetry, which means that the phosphatidylserine is carried from the inner membrane to the outer side. This event can be easily detected with annexin-V and can identify the apoptotic population in a particular cell population. Herein, we found that a good percentage of MCF-7 cells exposed to D-erythro-MAPP and its SLN formulation led to apoptosis in MCF-7 cells. The cell cycle analysis revealed that cell population on G1 stage was considerably decresed for both D-erythro-MAPP and D-erythro-MAPP SLN agents. The same finding was obtained for S and M stages that means slowing down the cell cycle and proliferation. These findings were supported with the detected changes on membrane potential (Figs. 12 and 13). Both of the agents changed the mithochondrial membrane potentials but this was more significantly reccorded in D-erythro-MAPP SLN applied MCF-7 cells that imply to apoptosis via mithochondrial dysfunction caused by the applied agents. Parallelly with our findings Colombini (2010) in a study showed how ceramide induces mitochondrial dysfunction, leading to apoptosis. Research data revealed that ceramide accumulate in the outer mitochondrial membrane and cause big channels for release of apoptotic proteins that initiate apoptosis irreversibly (Colombini 2010). The data also was underlined with our TEM and confocal microscopy findings that refer to the ultrastructural and morphological changes on the basis of apoptotic cell death.

Nowadays, the increasing number of cancer cases and the lack of exact treatment methods, the search for alternative treatment methods and the new treatment approaches to be obtained have attracted a lot of attention. The current treatment methods are insufficient and show side effects and encourages many scientists to make new researches. Recent studies on cancer have revealed the relationship of sphingolipid metabolism with cancer, and studies with ceramide, the basic molecule of sphingolipid metabolism, have become very popular. When the results obtained with this study are evaluated, more information about the effects of D-erythro-MAPP and its SLN formulation on the breast cancer cell line has been included in the literature. Our results are considered to provide a source and base for further studies for anticancer and therapeutic mechanisms of both agents on cancer treatment in vitro and in vivo. Moreover, results of this

study, will contribute to the next novel therapy approches via using targetted drugs on SLN basis, apart from various traditional cancer therapies.

Acknowledgements This study was supported by The Scientific and Technological Research Council of Turkey (TÜBİTAK) with Project number 118Z943.

Compliance with ethical standards

Conflict of interest Authors claim no conflicts of interest for this research.

References

Akar U, Chaves-Reyez A, Barria M, Tari A, Sanguino A, Kondo Y, Kondo S, Arun B, Lopez-Berestein G, Ozpolat B (2008) Silencing of Bcl-2 expression by small interfering RNA induces autophagic cell death in MCF-7 breast cancer cells. Autophagy 4:669–679

Ateş H (2015) Nano Parçacıklar ve Nano Teller. Gazi Üniversitesi Fen Bilimleri Dergisi C 3:437–442

Baul U, Uddhav SB, Vrushali P, Nachket V, Antara K (2018) Current status of solid lipid nanoparticles: a review. Mod Appl Boequiv Availab 3:1–2

Bhabak KP, Kleuser B, Huwiler A, Arenz C (2013) Effective inhibition of acid and neutral ceramidases by novel B-13 and LCL-464 analogues. Bioorg Med Chem 21:874–882

Bielawska A, Greenberg S, Perry D, Jayade S, Shayman JA, McKay C, Hannun YA (1996) (1S,2R)-D-erythro-2-(N-Myristoylamino)-1-phenyl-1-propanol as an inhibitor of ceramidase. J Biol Chem 271:12646–12654

Cengiz M, Ayhancı A, Kutlu HM, Musmul A (2016) Potential therapeutic effects of silymarin and silymarin-loaded solid lipid nanoparticle on experimental kidney damage in Balb/C mice: biochemical and histopathological evaluation. Turk J Biol 40:807–814

Ciftci GA, Işcan A, Kutlu HM (2015) Escin reduces cell proliferation and induces apoptosis on glioma and lung adenocarcinoma cell lines. Cytotechnology 67:893–904

Choi MS, Anderson MA, Zhang Z, Zimonjic DB, Popescu N, Mukherjee AB (2003) Neutral ceramidase gene: role in regulating ceramide-induced apoptosis. Gene 315:113-122

Colombini M (2010) Ceramide channels and their role in mitochondria-mediated apoptosis. Biochem Biophys Acta 1797:1239–1244

Cuvillier O (2002) Sphingosine in apoptosis signaling. Biochem Biophys Acta 1585:153–162

Das S, Chaudhury A (2011) Recent advances in lipid nanoparticle formulations with solid matrix for oral drug delivery. AAPS PharmSciTech 12:62–76

Draper JM, Xia Z, Smith RA, Zhuang Y, Wang W, Smith CD (2011) Discovery and evaluation of inhibitors of human ceramidase. Mol Cancer Ther 10:2052–2061

Erdogan A (2018) Magnetic nanoparticles in the diagnosis and treatment of cancer. Nat Appl Sci J 1:23–30

Hannun YA (1996) Functions of ceramide in coordinating cellular responses to stress. Science 274:1855–1859

Edmondson JM, Armstrong LS, Martinez A (1988) A rapid and simple Mtt-based spectrophotometric assay for determining drug ensitivity in monolayer cultures. J Tissue Cult Methods 11:15–17

Kim RH, Takabea K, Milstienb S, Spiegelb S (2009) Export and functions of sphingosine-1-phosphate. Biochim Biophys Acta 1791:692–696

Koçak S, Çelik L, Özbaş S, Dizbay SS, Tükün A, Yalçın B (2011) Meme Kanserinde Risk Faktörleri, Riskin Değerlendirilmesi ve Prevansiyon: İstanbul 2010 Konsensus Raporu. J Breast Health 7:47–67

Müller RH, Radtke M, Wissing SA (2002a) Nanostructured lipid matrices for improved microencapsulation of drugs. Int J Pharm 242:121–128

Müller RH, Radtke M, Wissing SA (2002b) Solid lipid nanoparticles (SLN) and nanostructured lipid carriers (NLC) in cosmetic and dermatological preparations. Adv Drug Deliv Rev 54:S131–S155

Natalie AF, Peng S, Cheng K, Sun S (2009) Magnetic nanoparticles: synthesis, functionalization, and applications in bioimaging and magnetic energy storage. Chem Soc Rev 38:2532–2542

Ogretmen B (2018) Sphingolipid metabolism in cancer signalling and therapy. Nat Rev Cancer 18:33

Ogretmen B, Hannun YA (2004) Biologically active sphingolipids in cancer pathogenesis and treatment. Nat Rev Cancer 4:604–616

Oskouian B, Saba JD (2010) Cancer treatment strategies targeting sphingolipid metabolism. Adv Exp Med Biol 688:185–205

Riboni L, Campanella R, Bassi R, Villani R, Gaini SM, Martinelli-Boneschi F, Viani P, Tettamanti G (2002) Ceramide levels are inversely associated with malignant progression of human glial tumors. Glia 39:105–113

Siegel R, Ma J, Zou Z, Ahmedin J (2014) Cancer statistics. CA Cancer J Clin 64:9–29

Vejselova D, Kutlu HM, Kuş G, Kabader S, Uyar R (2014) Cytotoxic and apoptotic effects of ceranib-2 offering potential for a new antineoplastic agent in the treatment of cancer cells. Turk J Biol 38:916–921

Vejselova D, Kutlu HM, Kus G (2016) (2016) Examining impacts of ceranib-2 on the proliferation, morphology and ultrastructure of human breast cancer cells. Cytotechnology 68:2721–2728

Venkateswarlu V, ManJunath K (2004) Preparation, characterization and in vitro release kinetics of clozapine solid lipid nanoparticles. J Control Release 95:627–638

Vethakanraj HS, Babu TA, Sudarsanan GB, Duraisamy PK, Kumar SA (2015) Targeting ceramide metabolic pathway induces apoptosis in human breast cancer cell lines. Biochem Biophys Res Commun 464:833–839

Westesen K (2000) Novel lipid-based colloidal dispersions as potential drug administration systems ± expectations and reality. Colloid Polym Sci 278:608–618

Wissinga SA, Kayser O, Mullerb RH (2004) Solid lipid nanoparticles for parenteral drug delivery. Adv Drug Deliv Rev 56:1257–1272

Yang HL, Chen CS, Chang WH, Lu FJ, Lai YC, Chan CC (2006) Growth inhibition and induction of apoptosis in MCF7 breast cancer cells by Antrodia camphorata. Cancer Lett 231:215–227

Zdzislaw M, Szulc NM, AiPing B, Bielawski J, Xiang L, James S, Yusuf A, Alicja B (2008) Novel analogs of D-ef-MAPP and B13. Part 1: synthesis and evaluation as potential anticancer agents. Bioorg Med Chem 16:1015–1031